Parameterization-free Projection for Geometry Reconstruction

Yaron Lipman Daniel Cohen-Or David Levin Hillel Tal-Ezer
Tel-Aviv University Academic College
of Tel-Aviv Yaffo

Abstract

We introduce a Locally Optimal Projection operator (LOP) for surface approximation from point-set data. The operator is parameterization free, in the sense that it does not rely on estimating a local normal, fitting a local plane, or using any other local parametric representation. Therefore, it can deal with noisy data which clutters the orientation of the points. The method performs well in cases of ambiguous orientation, e.g., if two folds of a surface lie near each other, and other cases of complex geometry in which methods based upon local plane fitting may fail. Although defined by a global minimization problem, the method is effectively local, and it provides a second order approximation to smooth surfaces. Hence allowing good surface approximation without using any explicit or implicit approximation space. Furthermore, we show that LOP is highly robust to noise and outliers and demonstrate its effectiveness by applying it to raw scanned data of complex shapes.

Keywords: point-cloud, surface reconstruction, geometry, projection operator

1 Introduction

Reconstructing the geometry of a shape from scanned data has been an important research objective in the last two decades [Hoppe et al. 1992; Amenta et al. 1998; Levoy et al. 2000; Kazhdan et al. 2006]. Despite the proliferation of surface reconstruction techniques, many aspects of the problem remain open. Two prominent difficulties in the reconstruction process are shape complexity and noise. Surface reconstruction methods (e.g., [Hoppe et al. 1992; Alexa et al. 2001; Carr et al. 2001; Ohtake et al. 2003; Amenta and Kil 2004; Kazhdan et al. 2006]) work well when the data is densely sampled and the orientation of the points can be deduced from the samples themselves. In the case of complex geometry (e.g., Figure 1) the surface cannot be reasonably approximated by a simple oriented manifold, that is, it cannot be well parameterized and approximated over a local plane. Such a scenario, for example, is manifested in thin parts where two folds of the shape are close to each other and the noise level is high. Therefore, augmenting the data points with orientation, either by supplying normals or off-surface points, is an extremely hard task.

Reconstruction by a projection operator has an important virtue: It defines a consistent geometry based on the data points, and provides constructive means to up-sample it. For example, the MLS projection operator [Levin 2003] has been established as a powerful surface reconstruction technique. However, the MLS

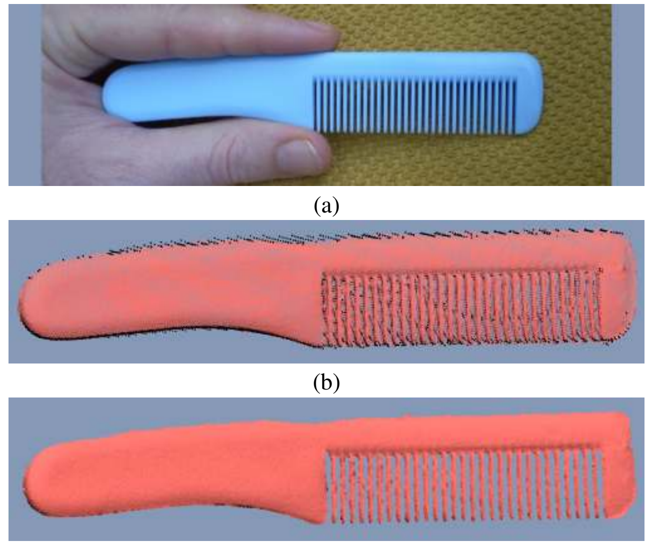

(a)

(b)

(b)

Figure 1: (a) A photograph of the scanned comb. (b) Five registerated scans. (c) LOP reconstruction.

projector assumes that a local plane can well approximate the data locally. In this context it is desirable to devise a projection operator which can efficiently deal with complex geometry. In particular, such an operator should not insist on using local orientation information such as reference planes or normals.

In this paper, we introduce a parameterization-free local projection operator (LOP). Apparently, it uses a more primitive projection mechanism, but since it is not based on a local 2D parameterization, it is more robust and operates well in complex scenarios. Furthermore, if the data points are locally sampled from a smooth surface, the operator provides a second order approximation, leading to a plausible approximation of the sampled surface. The new projection operator is introduced via a certain fixed-point iteration, where the approximated geometry consists of its stationary points. The origin of the method is Weiszfeld's algorithm for the solution of the Fermat-Weber point-location problem, also known as the multivariate L_1 median. This is a statistical tool which is traditionally applied globally to multivariate non-parametric point-samples, to generate a good representative for a large number of samples in the presence of noise and outliers. The problem was first known as the optimal location problem of Weber [1909]. The task was to find an optimal location for an industrial site that minimizes access cost. In statistics, the problem is known as L_1 median [Brown 1983; Small 1990]. Weiszfeld [1937] suggested a simple iterative procedure for computing the L_1 median. Later, Kuhn [1973] gave Weiszfeld's algorithm a rigorous treatment, and also noted that the problem goes back to Fermat in the early 17th century. The Fermat-Weber (global) point-location problem is considered as a spatial median since, if restricted to the univariate case, it coincides with the univariate median, and it inherits several of its properties in the multivariate setting. In this work, we apply this tool locally in a geometric context to constitute a robust mechanism

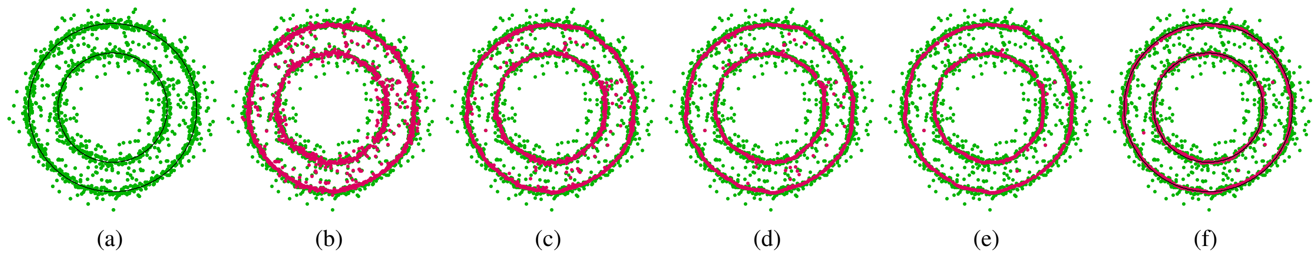

Figure 2: Iterative projection of a 2D noisy data taken from two concentric circles of radii 0.7 and 1.0 (a) (illustrated with thin black circles), using a large influence radius $h = 0.7$. (b),(c),(d),(e),(f) show the projected set after 1,3,5,10,20 iterations, respectively. Note the few remaining "floating points", which can be removed by local analysis, see Section 2. Moreover, note that the expected shrinkage effect is insignificant (f).

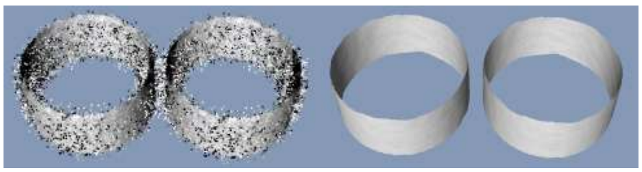

Figure 3: Nearly osculatory cylinders. Left: the input data. Right: LOP reconstruction.

for geometry reconstruction. Our approach is also related to the so-called "running median" method for filtering time series or images. However, LOP is a projection operator rather than a filter, and unlike the running median it requires no local parameterization.

LOP operator has two immediate functionalities: Firstly, it can be used as a preprocess stage for any other higher-order reconstruction technique (e.g., RBF). LOP can be applied on raw scanned data to create a clean data-set, as a means of efficiently reducing noise and outliers, and of simplifying the determination of a local surface orientation and topology. Secondly, it can be used to refine a given dataset. In the following, we show the results of applying LOP operator to a number of raw datasets, where the complexity of the models is particularly challenging.

2 Locally Optimal Projection - LOP

Given the data point-set $P = \{p_j\}_{j\in J} \subset \mathbf{R}^3$, LOP projects an arbitrary point-set $X^{(0)} = \{x_i^{(0)}\}_{i\in I} \subset \mathbf{R}^3$ onto the set P, where I, J denote the indices sets. We would like to define the set of projected points $Q = \{q_i\}_{i\in I}$ such that it minimizes the sum of weighted distances to points of P, with respect to radial weights centered at the same set of points Q. Furthermore, the points Q should not be too close to each other. This framework induces the definition of the desired points Q as the fixed point solution of the equation

$$Q = G(Q), \tag{1}$$

where

$$\begin{aligned} &G(C) = \mathrm{argmin}_{X=\{x_i\}_{i\in I}}\{E_1(X,P,C)+E_2(X,C)\}, \\ &E_1(X,P,C) = \textstyle\sum_{i\in I}\sum_{j\in J}\|x_i - p_j\|\theta(\|c_i - p_j\|), \\ &E_2(X,C) = \textstyle\sum_{i'\in I}\lambda_{i'}\sum_{i\in I\setminus\{i'\}}\eta(\|x_{i'} - c_i\|)\theta(\|c_{i'} - c_i\|). \end{aligned} \tag{2}$$

Here $\theta(r)$ is a fast-decreasing smooth weight function with compact support radius h defining the size of the influence radius, $\eta(r)$ is another decreasing function penalizing $x_{i'}$ which get too close to other points, and $\{\lambda_i\}_{i\in I}$ are balancing terms, which we denote by Λ. In a nutshell, the term E_1 drives the projected points Q to approximate the geometry of P, and the term E_2 strives at keeping the distribution of the points Q fair. In the following, we explain each of the two terms, and then we show that proper values Λ can guarantee second order approximation power of LOP operator given that the data is sampled from a C^2 surface.

L_1 median. The first cost function E_1 is closely related to the multivariate median, also referred to as the L_1 median. Given a data set P, the L_1 median is defined as the point q, minimizing the sum of Euclidean distances to the data points:

$$q = \underset{x}{\mathrm{argmin}}\left\{\sum_{j\in J}\|p_j - x\|\right\}. \tag{3}$$

It is known that, unlike the usual (mean) average, the "L_1" median is not sensitive to the presence of outliers in the data. E_1 can be seen as a localized version of the cost function in (3) which aims to obtain from P local approximations to the underlying geometry: Instead of looking for one point q representing all the data points P, we look for set of points $Q = \{q_i\}_{i\in I}$ which represent the geometry. We localize the cost function using a fast-decaying weight function θ with the finite support radius h (we used the approximation $\theta(r) = e^{-r^2/(h/4)^2}$). The solution of

$$Q = \underset{X}{\mathrm{argmin}}\, E_1(X,P,Q) \tag{4}$$

can be interpreted as being the set Q of *local* 'distribution centers'.

Regularization. The solution of (4) produces good approximations to points on the surface, but the resulting points Q have an irregular spatial distribution and tend to accumulate in clusters. The second cost function $E_2(X,Q)$ regularizes the points in Q by incorporating local repulsion forces. We generally use the repulsion functions of the form $\eta(r) = 1/3r^3$. As in other minimization problems involving the sum of two cost functions, it is important to set appropriate values to the parameters Λ in (2). Small values of Λ enforce good approximation at the expense of poor distribution. On the other hand, large values of Λ gives weight to a data independent term, which only strives for a fair distribution of the points. As we will show next, there is a choice of Λ which guarantees LOP having an $O(h^2)$ approximation order, where h is the support size of the weight function θ.

Approximation order of LOP. An important property of LOP operator is the ability to approximate surfaces without any local orientation information nor a local manifold assumption. An important parameter which plays a major role in the application of LOP is h, the support size of the weight function θ. The following theorem guarantees an $O(h^2)$ approximation order, which is asymptotic as $h \to 0$. As a by-product of the approximation order analysis, we shall also derive the proper choice of balancing parameters Λ in the computational LOP procedure.

Theorem 2.1. *If the data set P is sampled from a C^2-smooth surface S, LOP operator has an $O(h^2)$ approximation order to S, provided that Λ is carefully chosen.*

Proof. In letting h tend to zero we assume that the number of projected points, I, is fixed, while the number of input points, J, may grow. $G(C)$, as defined in (2), satisfies $\nabla_X|_{X=G(C)}(E_1(X,P,C)+E_2(X,C)) = 0$. Therefore, the points $Q = \{q_i\}_{i\in I}$ defined by Eq. (1) satisfying $\nabla_X|_{X=Q}(E_1(X,P,Q)+E_2(X,Q)) = 0$, which leads to the relation:

$$\sum_{j\in J}(q_{i'}-p_j)\alpha_j^{i'} - \lambda_{i'}\sum_{i\in I\setminus\{i'\}}(q_{i'}-q_i)\beta_i^{i'} = 0\ , \quad i'\in I, \tag{5}$$

where $\alpha_j^{i'} = \frac{\theta(\|q_{i'}-p_j\|)}{\|q_{i'}-p_j\|}$, $j\in J$ and $\beta_i^{i'} = \frac{\theta(\|q_{i'}-q_i\|)}{\|q_{i'}-q_i\|}\left|\frac{\partial\eta(\|q_{i'}-q_i\|)}{\partial r}\right|$, $i\in I\setminus\{i'\}$. Note that we have used the fact that η is decreasing, that is, its derivative is always negative. After rearranging and setting $\lambda_{i'} = \mu\frac{\sum_{j\in J}\alpha_j^{i'}}{\sum_{i\in I\setminus\{i'\}}\beta_i^{i'}}$, $\mu > 0$, we get

$$(1-\mu)q_{i'} + \mu\sum_{i\in I\setminus\{i'\}} q_i\frac{\beta_i^{i'}}{\sum_{i\in I\setminus\{i'\}}\beta_i^{i'}} = \sum_{j\in J} p_j\frac{\alpha_j^{i'}}{\sum_{j\in J}\alpha_j^{i'}}\ , \quad i'\in I. \tag{6}$$

Viewing (6) as a system of equations for Q,

$$AQ = R, \tag{7}$$

Note that both A and R are also depending on Q, yet, by analyzing A^{-1} and R we show below that $Q = A^{-1}R$ are points at distance $O(h^2)$ from the surface S. The proof is by showing that each $q_{i'}$ is an average of nearby points, on the surface or near it. We shall use the observation that an affine average of points on a plane is also on that plane, and that the surface can be locally approximated by a plane, with an approximation error of $O(h^2)$. The sum on the r.h.s. of (6) represents a local convex combination of points within a distance h from $q_{i'}$. We may assume that this sum is not empty. Otherwise, by (6) it follows that $q_{i'}$ is at, or near, the origin, and such points will be discarded. Thus, using the local plane reconstruction property of affine combinations, we have that the r.h.s. equals $F+O(h^2)$, where $F = \{f_{i'}\}_{i'\in I}$ are points on S. Also, due to the finite support of θ, we further have $|f_i - q_i| \le h + O(h^2)$. Next, we have $AQ = F + O(h^2)$. If we take $\mu\in[0,1/2)$, then A is strictly diagonally dominant and therefore we can bound $\|A^{-1}\|_\infty \le \frac{1}{1-\mu}\sum_{k=0}^{\infty}(\frac{\mu}{1-\mu})^k = \frac{1}{1-2\mu}$. Now, since the rows of A sum up to one, so do the rows of A^{-1}. Furthermore, we note that $|(A^{-1})_{\ell,m}| \le a_1(\frac{\mu}{1-\mu})^k$ when the distance between q_ℓ and q_m is greater or equal to kh; that is, the influence of distant points decays exponentially with distance. The above implies that $Q = A^{-1}F + O(h^2)$, and each element $(A^{-1}F)_{i'}$ is an affine average of f_i on the surface, with weights exponentially decaying with the distance $\|f_{i'} - f_i\|$. Let T be the tangent plane to S at $f_{i'}$, and let $f_i = t_i + r_i$ where t_i is the projection of f_i on T. It can be shown that $\|r_i\| < a_2\|f_i - f_{i'}\|^2$. Then $(A^{-1}F)_{i'} = \sum_{i\in I}A^{-1}_{i',i}(t_i + r_i) = \sum_{i\in I}A^{-1}_{i',i}t_i + \sum_{i\in I}A^{-1}_{i',i}r_i$. We would first like to show that $\|\sum_{i\in I}A^{-1}_{i',i}t_i - f_{i'}\| = O(h)$ and since $\sum_{i\in I}A^{-1}_{i',i}t_i$ is on T it will follow that it is an $O(h^2)$ distant from S. Secondly, we will show $\sum_{i\in I}A^{-1}_{i',i}r_i = O(h^2)$. This will show that $(A^{-1}F)_{i'}$ and consequently $q_{i'}$ is $O(h^2)$ distant from S. Then, for a fixed i' let us denote by I_k the set of indices of points q_i such that $\|q_i - q_{i'}\| \in [kh,(k+1)h)$. $\left\|\sum_{i\in I}A^{-1}_{i',i}t_i - f_{i'}\right\| = \left\|\sum_{i\in I}A^{-1}_{i',i}(t_i - f_{i'})\right\| \le$

$$\sum_{k\ge0}\sum_{i\in I_k}a_1(\tfrac{\mu}{1-\mu})^k((k+1)h + O(h)) = O(h). \tag{8}$$

Next, in the same way, using the observation that $\|r_i\| < a_2((k+1)h + O(h))^2$, for $i\in I_k$, we conclude that $\|\sum_{i\in I}A^{-1}_{i',i}r_i\| = O(h^2)$. □

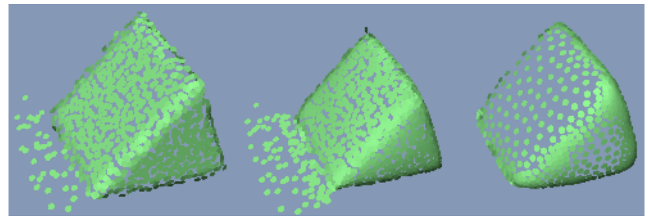

Figure 4: Left: A prism point-cloud contaminated with ghost-geometry noise. Middle: MLS. Right: LOP. In both the point-set is projected onto itself.

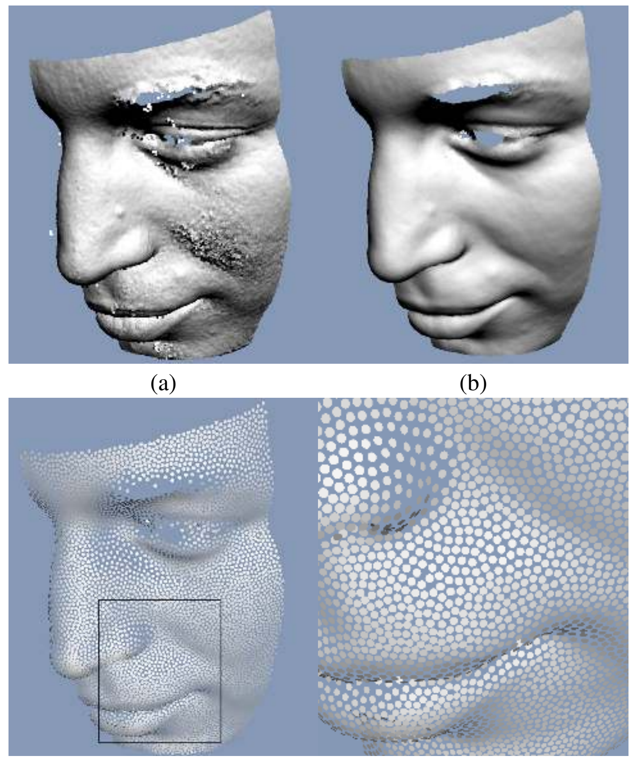

(a) (b)

(c) (d)

Figure 5: The point-cloud in (a) consists of three registered scans. (b) LOP reconstruction. (c-d) show the quality of the points' distribution of LOP projection, where 1/16 of the original point number is used.

The iterative LOP algorithm. The above leads to an iterative solution to (1) which guarantees an $O(h^2)$ approximation order: Fix a repulsion parameter $\mu\in[0,1/2)$. Next, define $X^{(1)} = \{x_i^{(1)}\}_{i\in I}$ by

$$x_{i'}^{(1)} = \frac{\sum_{j\in J}p_j\theta(\|p_j - x_{i'}^{(0)}\|)}{\sum_{j\in J}\theta(\|p_j - x_{i'}^{(0)}\|)}\ , \quad i'\in I.$$

Then, at each iteration $k = 1,2,3,\ldots$ define for $i'\in I$

$$\alpha_j^{i'} = \frac{\theta(\|x_{i'}^{(k)} - p_j\|)}{\|x_{i'}^{(k)} - p_j\|}\ ,\ \beta_i^{i'} = \frac{\theta(\|x_{i'}^{(k)} - x_i^{(k)}\|)}{\|x_{i'}^{(k)} - x_i^{(k)}\|}\left|\frac{\partial\eta}{\partial r}(\|x_{i'}^{(k)} - x_i^{(k)}\|)\right|$$

for $i\in I\setminus\{i'\}$. Then, by rearranging (6) we derive our fixed point iterations as

$$x_{i'}^{(k+1)} = \sum_{j\in J}p_j\frac{\alpha_j^{i'}}{\sum_{j\in J}\alpha_j^{i'}} + \mu\sum_{i\in I\setminus\{i'\}}\left(x_{i'}^{(k)} - x_i^{(k)}\right)\frac{\beta_i^{i'}}{\sum_{i\in I\setminus\{i'\}}\beta_i^{i'}},$$

for every $i' \in I$. Upon convergence, the limit satisfies the necessary condition (5), and by Theorem 2.1 the approximation order is guaranteed. Figure 2 exhibits a 2D example of the iterative process. There could be a small number of points which LOP operator might not project as expected. There are two typical scenarios: (i) The point's distance from the surface is larger than the support size of the influence weight function θ, that is h. (ii) The point is exactly midway between two attractors; for example, see Figure 2 (f). In both cases these problematic points can easily be detected via a local points' distribution analysis, since the weighted density in the vicinity of such points is smaller than the density of the points on the surface. In our implementation we detect these points using a parameter and discard them.

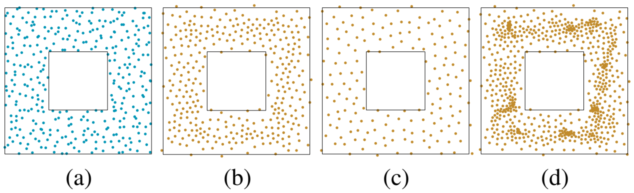

Figure 6: Up-sample/down-sample example. A planar point-cloud (a) was projected onto itself using LOP (b). (c) shows projection of a halved set onto the original data (a) (down-sample). (d) shows projection of doubled set (up-sample).

Application of LOP. LOP can be used to project an arbitrary set of points $X^{(0)}$ onto an input point-cloud P. We observe that taking $X^{(0)}$ with less points than P results in more regular distribution of projected points, see Figure 6 and 5(c–d). The rationale is that the input data can be regarded as consisting of multiple observation of the same data (e.g., multiple registered scans), and LOP operator generates a concise set of points that represents well the input data. In a sense, it operates like a multivariate median, which defines a representative to a set of samples. Then, to up-sample the initial projection, we enriched the above projected set and performed few ($\approx$ 3 or 4) iterations of LOP. It is important to note that LOP is rather independent of the initial guess $X^{(0)}$. See Figure 8 where an initial crude guess results in a fair and faithful approximation. LOP algorithm is controlled by two parameters: h and μ. To study their influence on the properties of the projected set Q, see Figure 12. h is the local influence size of the operator; it is usually best to start the iterations with h as large as the expected outliers magnitude and then refine h as the iterations progress. Similarly, one can start with a small μ and then increase it. μ reflects the tradeoff between accuracy ($\mu \in [0.1, 0.25]$) and regular distribution ($\mu \in [0.3, 0.45]$).

3 Results and conclusions

Figures 1, 5, 7, 10 show the results of applying LOP to raw data-sets acquired by a scanner. For each model a number of scans are registered, forming a noisy and incomplete point-cloud. The shape of the models that we use are challenging. Figure 3 shows a synthetic example where the correct topology of two near osculatory cylinders is reconstructed by LOP. Figures 4, 9, 10 and 11 show different comparisons of LOP and MLS. All the examples are rendered using PointShop3D [Zwicker et al. 2002]. The normals used for shading are computed with the same local PCA algorithm. In Figure 10 we used voxel data extracted from multi-view video.

The algorithm requires typically 20 iterations of averaging for projecting a point-set onto itself. An exception is the example depicted in Figure 8, where the initial guess $X^{(0)}$ is very crude,

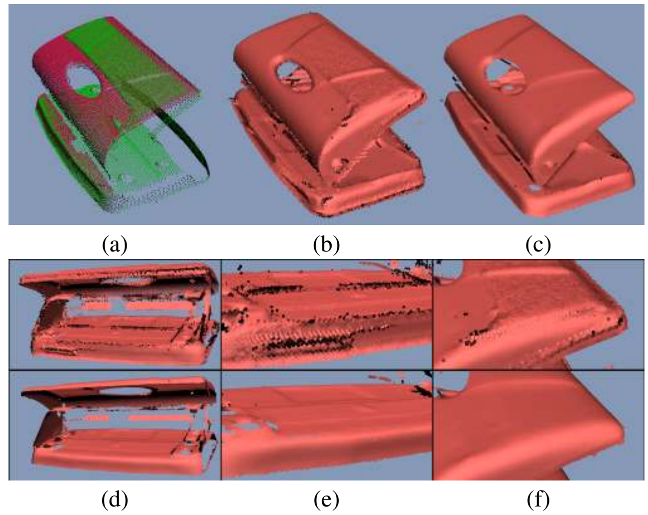

Figure 7: Hole-puncher scan which consists of a few registered scans suffering from bad alignment, noise and outliers. (a) shows an example of two scans which where registered using ICP. (b),(d-top) are the whole input data seen from two angles. Note the high noise and ghost geometry. The corresponding LOP reconstruction is depicted in (c),(d-bottom). Note the zoomed-in views in (e) and (f).

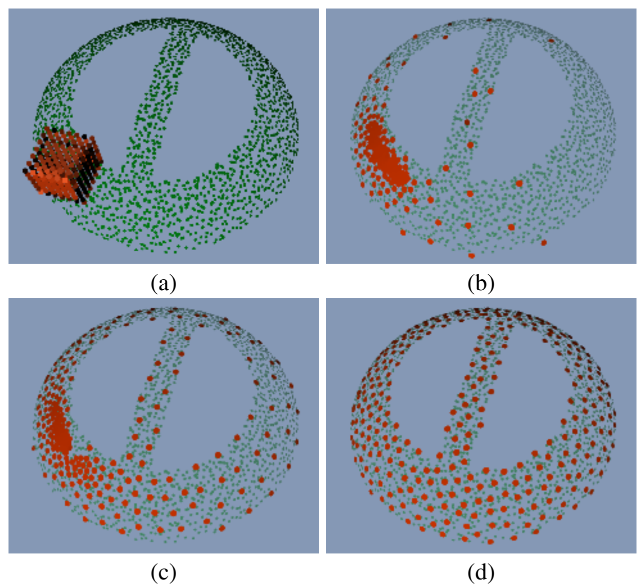

Figure 8: This example depicts the distribution of point by LOP operator. (a): Starting from a crude initial guess (red points projected onto the green point-set), the operator iteratively (b–d) distribute the points regularly while respecting the geometry faithfully.

and the algorithm required several hundred iterations. After enriching the projected set we performed few iterations only. We implemented the algorithm in MATLAB with no optimization; it projects approximately 200 points a second (the timing depends on h) in the first stage, and 1000 points a second in the up-sampling.

The current notable limitation of LOP reconstruction algorithm is the use of a local density parameter h. Although such a parameter exists in many reconstruction techniques, we believe that it is important to avoid any use of parameters. As we demonstrate in Figure 2, LOP operator has only little shrinkage effect, if any. This

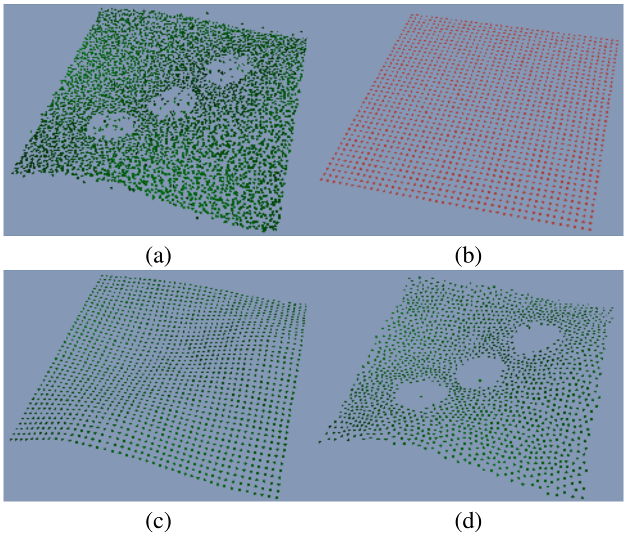

Figure 9: A noisy point-cloud of a surface with three holes (a). The red points in (b) are projected onto the point-set in (a). The results of the MLS and LOP projections are shown in (c),(d), respectively.

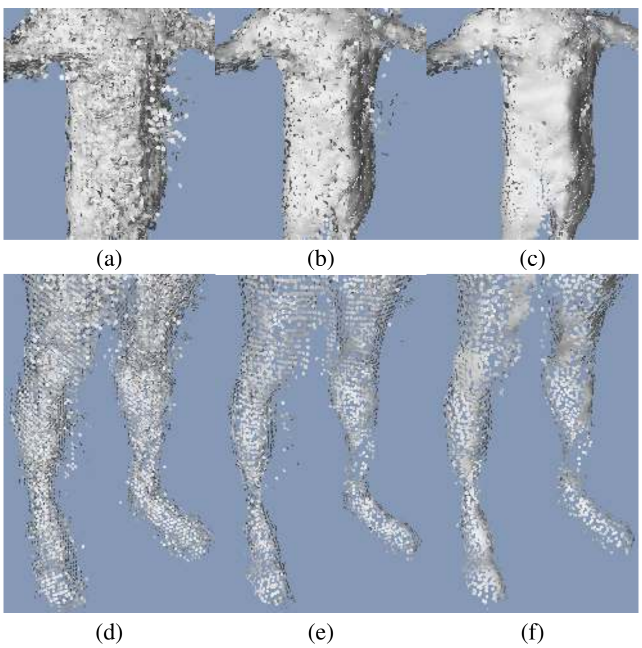

Figure 10: Five low-resolution and noisy voxel multi-view scans of a dancer are registered (a),(d). (b) and (e) show a projection of a smaller set using MLS. (c),(f) show the projection of the same set using LOP.

can be attributed to the fact that the convex averaging effect of E_1 is balanced by the repulsion effect of E_2. A challenging future work is trying to deduce the optimal parameter h from the data itself, and further analyzing the convergence of the iterative process.

Acknowledgements We would like to thank Craig Gotsman and Alexander Bogomjakov for the granted access to their scan facilities, and Christian Theobalt for supplying the dancer data. This work was supported by the Israel Science Foundation.

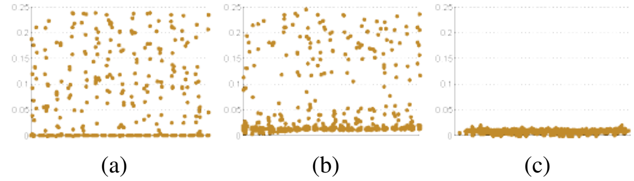

Figure 11: A point-cloud of a plane with one-sided 50% noise (viewed from the side). (a) is the data. (b),(c) shows MLS, LOP projection of the set onto itself with $h = 0.5$, respectively.

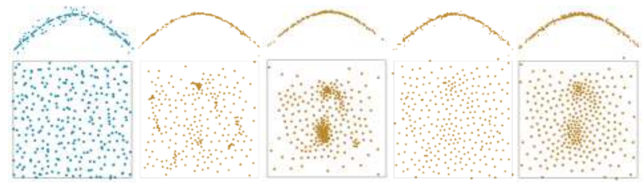

data	$\mu = 0.25$ $h = 0.5$	$\mu = 0.25$ $h = 0.7$	$\mu = 0.45$ $h = 0.5$	$\mu = 0.45$ $h = 0.7$

Figure 12: A curved surface patch with 50% noise is projected onto itself with different h, μ values. The two rows show up and side views. The squares are of dimension $[0,1]^2$.

References

ALEXA, M., BEHR, J., COHEN-OR, D., FLEISHMAN, S., LEVIN, D., AND SILVA, C. T. 2001. Point set surfaces. In *VIS '01: Proceedings of the conference on Visualization '01*, 21–28.

AMENTA, N., AND KIL, Y. J. 2004. Defining point-set surfaces. *ACM Trans. Graph. 23*, 3, 264–270.

AMENTA, N., BERN, M., AND KAMVYSSELIS, M. 1998. A new voronoi-based surface reconstruction algorithm. ACM Press, New York, NY, USA, 415–421.

BROWN, B. M. 1983. Statistical uses of the spatial median. *J. R. Stat. Soc. 45*, 1, 25–30.

CARR, J. C., BEATSON, R. K., CHERRIE, J. B., MITCHELL, T. J., FRIGHT, W. R., MCCALLUM, B. C., AND EVANS, T. R. 2001. Reconstruction and representation of 3d objects with radial basis functions. In *SIGGRAPH '01*, 67–76.

HOPPE, H., DEROSE, T., DUCHAMP, T., MCDONALD, J., AND STUETZLE, W. 1992. Surface reconstruction from unorganized points. *Computer Graphics 26*, 2, 71–78.

KAZHDAN, M., BOLITHO, M., AND HOPPE, H. 2006. Poisson surface reconstruction. In *Symposium on Geometry Processing*, 61–70.

KUHN, H. W. 1973. *Math. Program. 4*, 98–107.

LEVIN, D. 2003. Mesh-independent surface interpolation. *Geometric Modeling for Scientific Visualization*, 37–49.

LEVOY, M., PULLI, K., CURLESS, B., RUSINKIEWICZ, S., KOLLER, D., PEREIRA, L., GINZTON, M., ANDERSON, S., DAVIS, J., GINSBERG, J., SHADE, J., AND FULK, D. 2000. The digital michelangelo project: 3d scanning of large statues. In *SIGGRAPH '00*, 131–144.

OHTAKE, Y., BELYAEV, A., ALEXA, M., TURK, G., AND SEIDEL, H.-P. 2003. Multi-level partition of unity implicits. *ACM Trans. Graph. 22*, 3, 463–470.

SMALL, C. G. 1990. A survey of multidimensional medians. *Int. Stat. rev. 58*, 3, 263–277.

WEBER, A. 1909. *[translated by Carl J. Friedrich from Weber's 1909 book]. Theory of the Location of Industries. Chicago: The University of Chicago Press, 1929.*

WEISZFELD, E. 1937. Sur le point pour lequel la somme des distances de points dennes est minimum. *Tohoko Math. J. 43*, 355–386.

ZWICKER, M., PAULY, M., KNOLL, O., AND GROSS, M. 2002. Pointshop 3d: an interactive system for point-based surface editing. *ACM Trans. Graph. 21*, 3, 322–329.